

See discussions, stats, and author profiles for this publication at: <https://www.researchgate.net/publication/253646691>

Dual-Aptamer-Based Biosensing of Toxoplasma Antibody

ARTICLE *in* ANALYTICAL CHEMISTRY · JULY 2013

Impact Factor: 5.64 · DOI: 10.1021/ac401755s · Source: PubMed

CITATIONS

11

READS

80

5 AUTHORS, INCLUDING:



Yang Luo

Third Military Medical University

22 PUBLICATIONS 218 CITATIONS

SEE PROFILE



Xing xing Liu

Nanjing Normal University

18 PUBLICATIONS 170 CITATIONS

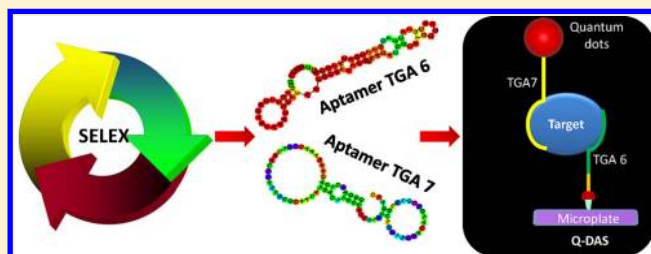
SEE PROFILE

Dual-Aptamer-Based Biosensing of Toxoplasma Antibody

Yang Luo,^{*,†,‡,⊥} Xing Liu,^{†,⊥} Tianlun Jiang,[‡] Pu Liao,^{*,§} and Weiling Fu^{*,†}[†]Department of Laboratory Medicine, and [‡]Department of Transfusion Medicine, Southwest Hospital, the Third Military Medical University, Chong Qing 400038, China[§]Clinical Laboratory Center of Chongqing, Chongqing 400014, China

S Supporting Information

ABSTRACT: A panel of seven aptamers to antitoxoplasma IgG is first discovered in this report. The aptamers are selected using systematic evolution of ligands by exponential enrichment (SELEX) technology, cloned, and identified by sequencing and affinity assay. Among them, two aptamers (TGA6 and TGA7) with the highest affinities are employed as capture probe and detection probe in developing a quantum dots-labeled dual aptasensor (Q-DAS). In the presence of antitoxoplasma IgG, an aptamer–protein–aptamer sandwich complex (TGA6–IgG–TGA7) is formed and captured on a multiwell microplate, whose fluorescence can be read out using quantum dots as the fluorescence label, ensuring highly sensitive and specific sensing of antitoxoplasma IgG. The operating characteristics of the proposed assay are guaranteed using dual aptamers as the recognizing probes when compared with antibody-based immunoassay. Q-DAS has a linearity within the range of 0.5–500 IU with a lowest detection of 0.1 IU. Receiver operating curves of 212 clinical samples show a 94.8% sensitivity and 95.7% specificity when the cutoff value is set as 6.5 IU, indicating the proposed Q-DAS is a promising assay in large-scale screening of toxoplasmosis.



Infection by *Toxoplasma gondii* during pregnancy is one of the leading causes of spontaneous abortion, fetal death, and birth defects worldwide. The overall seroprevalence of toxoplasma infection is estimated to be 22.5% in the United States and even up to 75% in El Salvador.¹ Toxoplasmosis can even be life threatening in immune-compromised individuals, such as AIDS patients and pregnant women.² Early diagnosis of toxoplasmosis provides the most effective means in reducing morbidity and mortality.

Toxoplasmosis can be recognized in laboratory either directly by polymerase chain reaction (PCR), DNA hybridization, histology, or indirectly by serological methods.^{3–5} Although direct demonstration of *T. gondii* in blood and urine could make a definitive diagnosis in congenital infections, negative results cannot exclude latent infections.⁶ PCR-based assays for *T. gondii* DNA determination identify live organisms with rapid speed, but their clinical applications are also hindered by both false-positive and false-negative results.⁷ Considering that live *T. gondii* are rarely detected in toxoplasmosis patients, serological examinations with the capability to detect toxoplasma-specific IgG antibodies are clinically adopted in assisting toxoplasma diagnosis. Among these immunoassays, Sabin–Feldman dye test (DT) is generally considered the gold standard method for toxoplasma antibodies detection. But it is only performed in specialized laboratories because of the consideration of potential risk from live virulent *T. gondii*.^{8–10}

Other antibody detection assays such as indirect fluorescent antibody test (IFA) and enzyme immunoassay have been developed and approved by the U.S. Food and Drug Administration to replace classical DT assay owing to

comparable results and the capability of automation in large numbers of specimens screening. But false-positive results have also been frequently documented due to the interference from various plasma proteins, such as antinuclear antibodies in toxoplasma-specific IgG detection and rheumatoid factor in IgM detection.¹¹ In addition, false-negative results are also reported in some initial infection cases. Microparticles-enhanced enzyme immunoassay provides an improved sensitivity and automation, but this approach still needs validation and standardization.¹² Recently, aptamer emerges as a promising molecular probe for protein or peptide detection. Compared with monoclonal antibody, aptamer has a higher dissociation constant with proteins, providing improved sensitivity and specificity.¹³ In addition, the aptamer-based assay provides satisfactory repeatability and cost-effectiveness because aptamers are easy to be synthesized via standardized chemical synthesis. Until now, series of aptamers have been selected for clinical detection of hepatitis C virus,¹⁴ *Bacillus anthracis*,¹⁵ ricin,¹⁶ and thrombin.¹⁷ But to our knowledge, no aptamers of toxoplasma antibodies have been reported until now.

In this experiment, we successfully discovered a panel of seven antitoxoplasma IgG aptamers for the first time, using systematic evolution of ligands by exponential enrichment (SELEX) technology. In addition, two aptamers with the highest affinity are employed to establish a quantum dots-

Received: June 12, 2013

Accepted: July 30, 2013

Published: July 30, 2013



labeled dual-aptasensor (Q-DAS) approach for ultrasensitive and high specific detection of antitoxoplasma IgG. By adopting two different aptamers as the capture probe and detection probe, respectively, the proposed Q-DAS assay provides significantly enhanced specificity when compared with conventional antibody-based assays.

■ EXPERIMENTAL SECTION

Chemicals and Reagents. Conventional reagents for PCR amplification (10× buffer, MgCl₂, Taq polymerase, dNTP) are from TaKaRa (Kyoto, Japan). Purification reagent (phenol/chloroform/isoamyl alcohol = 25:24:1) and protein-coated buffer (pH 9.6 carbonate buffer) are from Sigma-Aldrich (St. Louis, MO); bovine serum albumin (BSA), SELEX binding buffer (20 mmol/L Hepes pH 7.35, 120 mmol/L NaCl, 5 mmol/L KCl, 1 mmol/L CaCl₂, 1 mmol/L MgCl₂), SELEX washing buffer (0.05% Tween-20 plus SELEX binding buffer), SELEX eluting buffer (20 mmol/L Tris-HCl, 4 mol/L guanidine thiocyanate, 1 mmol/L DDT, pH 8.3), and PBST washing buffer (0.1 M PBS, pH = 7.4, with 0.05% Tween-20) are from Sigma-Aldrich (St. Louis, MO).

Antitoxoplasma monoclonal antibody and enzyme-labeled antibody are from Abcam (Cambridge, U.K.). The Qdot 565 ITK streptavidin conjugate kit was obtained from Invitrogen (Gaithersburg, MD). Purified human albumin, fibrinogen, vitamin B₁₂, high-density lipoprotein, chylomicrometers, immunoglobulin G, hemoglobin, glucose, and glutamate are purchased from Pierce (Rockford, IL). Corning DNA-BIND 96-well plates were obtained from Sigma-Aldrich (St. Louis, MO). A Synergy HT hybrid multimode microplate reader is obtained from BioTek (Winooski, VT) for fluorescence measurements. A microplate Genie mixer from Scientific Industries (Bohemia, NY) is used for reagent mixing.

Collection and Storage of Clinical Samples. A total of 145 negative samples are collected from healthy women (aged from 21.3 to 32.5 years old, with an average age of 26.7 years), and 67 positive samples are collected from pregnant women (aged from 24.2 to 35.7 years old, with an average age of 27.3 years). These participants are outpatients of Southwest Hospital between May 2009 and June 2012. All participants gave signed, informed consents, and this study was approved by the Ethics Boards of the Third Military Medical University. All serum samples have been verified by the DT assay. Blood was collected into BD Vacutainer tubes (New Jersey, U.S.A.) and centrifuged at 3000 rpm for 20 min for serum collection. All the collected serum samples are numbered and divided into two equal parts, then stored at −20 °C prior to detection with no freeze–thaw cycles before the protein assay.

Construction of the DNA Library. An aptamer library that consists of a random region of 35 nucleotides (GGGAGCTCA-GAATAAACGCTCA-N35-TTCGACATGAGGCCCGG-GATC) was applied as the original library. A forward primer of 5'-GGGAGCTCAGAATAAACGCTCA-3' and a reverse primer of 5'-biotin-TTCGACATGAGGCCCGGATC-3' was designed for PCR amplification of the ssDNA library. The ssDNA library and primers were synthesized by Shanghai Shenggong biological company (Shanghai, China), and the ssDNA library was prepared with streptavidin-immobilized gel beads. First the ssDNA library was amplified using optimized PCR parameters with the conditions containing ssDNA library 0.1 μg, 10× PCR buffer 2 μL, MgCl₂ of 1.5 mmol/L, forward primer 10 pmol, reverse primers 10 pmol, 0.2 mmol/L dNTP, Taq DNA polymerase 1 U; deionized water is added to a total

volume of 20 μL. An optimized working temperature cycle includes 94 °C for 300 s, 94 °C for 30 s, 65 °C for 30 s, 72 °C for 45 s. Next, asymmetric PCR was performed to construct the amplified ssDNA library, in which the optimized operating parameters are the same as those in the first PCR amplification cycle except for the ratio of forward primer and reverse primer. In a asymmetric PCR, 0.2 pmol of forward primer and 20 pmol of reverse primer were adopted to ensure most of the amplified nucleic acids molecules are single-strand DNA.

Aptamer Selection. Aptamer selection is conducted according to a previously reported SELEX protocol with a little modification.¹⁸ Briefly, antitoxoplasma IgG was immobilized on an assay plate for 3 h at 37 °C using carbonate buffer (pH 9.6), then 3% BSA was introduced into the microplate and incubated for 2 h. Meanwhile, another microplate that is coated with 3% BSA was prepared for counterselection. Then, any ssDNA sequence that can combine to BSA will be negative-selected by introducing the ssDNA library into the BSA-coated microplate, and the remaining ssDNA was washed into the microplate coated with antitoxoplasma IgG. After incubating for 1 h, the unbound ssDNA was removed by washing with SELEX washing buffer for six times. Then SELEX eluting buffer was introduced into the microplate at 80 °C for 10 min to dissolve the positive-selected ssDNA, followed by purification using purification reagent from Sigma-Aldrich. The purified ssDNA was amplified using PCR and asymmetric PCR, and the products were taken as the ssDNA library for the next SELEX cycle.

After approximately 10 SELEX cycles, the aptamers with high affinity to antitoxoplasma IgG can be obtained, which were subjected to cloning and identification consecutively. Mainly, the *Escherichia coli* DH5α competent cells were prepared and stored at −70 °C prior to use. Then, the selected ssDNA library was connected to the pMD18-T simple vector according to the protocol from TaKaRa. After incubation overnight at 16 °C, 20 μL of connection product was mixed with 100 μL of competent cells and ice-bathed for 30 min. Then 600 μL of SOC medium was introduced and incubated for 1 h to wait for the express of antibiotic-resistant marker labeled genes. The transformed DH5α competent cells were introduced into a LB plate containing 100 μg/mL ampicillin and incubated for 16 h at 37 °C. Then 110 randomly selected monoclonals were introduced into 600 μL of liquid medium containing 100 μg/mL ampicillin and cultured overnight with shaking at 200 rpm. Next, recombinant plasmid was extracted using kits from Qiagen. Then the ssDNA was amplified using asymmetrical PCR, and the ssDNA library was added into the wells coated by 1 μL/well antitoxoplasma IgG to test the affinity of selected aptamers.

For highly effective screening, the concentrations of ssDNA and toxoplasma antibody were optimized at every round. Then the SELEX cycle numbers were optimized using affinity selection experiments by measuring the absorbance at 450 nm. Meanwhile, those selected aptamer clones were sent for sequencing.

Primary Aptamer Coating on Microplates. Primary antitoxoplasma IgG aptamer coating was achieved by adding amine-modified aptamer into the DNA-BIND microplate. In a typical experiment, amine-modified TGA6 were diluted to 0.1 pmol/100 μL of coupling buffer (0.5 M Na₂HPO₄–NaH₂PO₄, pH 8.5) and divided into the wells of a DNA-BIND 96-well plate (100 μL per well). The wells were washed three times with wash buffer after incubating with gentle mixing for 40 min at 37 °C. Next, 300 μL of blocking buffer (washing buffer, pH 7.4,

with 2% BSA) was applied to each well for 2 h to ensure that all the remaining and available binding surfaces of the plastic wells were covered. Then, the microplates were dried and stored at 4 °C prior to use.

Preparation of the Quantum Dots–Aptamer Complex. The quantum dots (QD)–aptamer complex was prepared according to the procedure supplied by Invitrogen. Briefly, the biotin-labeled detection aptamer and the QD–streptavidin conjugate were mixed and incubated with slight stirring at 25 °C for 2 h to form the QD–aptamer complex. Next, the QD–aptamer complex was concentrated and purified prior to absorbance and fluorescence spectra measurement. A Bradford assay was performed to calculate the coupling efficiency by determining the amount of uncoupled aptamer. The conjugated aptamer concentration was determined by subtracting the amount of uncoupled aptamer from the total number of aptamers used in the assay. The induced concentrations of the QD–aptamer conjugate were determined accordingly.

Measurement Procedures. In each well of a microplate, 100 μ L of the solution (serum sample or diluted antitoxoplasma IgG standard) was incubated with the primary aptamer that was immobilized in the well at 25 °C for 20 min. Then each well was washed three times with PBST washing buffer at 2 min per wash. After incubating QD–aptamer complex with the microplate for 20 min, the microplate was washed three times with PBST washing buffer to remove any unreacted QD–aptamer complex prior to fluorescence measurement.

Methodological Evaluation and Clinical Sample Detection. Various analytical parameters, including the coated primary aptamer concentration (1–10 mg L⁻¹) and the concentrations of the QD-conjugated detection aptamer to antitoxoplasma IgG (0.1–1 mg L⁻¹), were optimized to achieve an ideal regression coefficient for the standard curve and a high signal-to-noise ratio of fluorescence intensity.

The operational characteristics, including the precision, specificity, analytical sensitivity, and detection limits, were evaluated to validate the proposed Q-DAS assay. All 212 clinical samples were analyzed for antitoxoplasma IgG levels using the Q-DAS sensor and dye test (Beckman, Brea CA), respectively. Receiver-operating characteristic (ROC) curve was performed with MedCalc (version 11.4) to analyze the sensitivity and specificity for clinical sample detection. A statistically significant difference between the fluorescence intensity induced by various interfering agents was tested with *t* tests. The calibration curves were plotted using Origin (version 8.6). Statistical analyses were performed using SPSS 20.0 software (SPSS Inc. Chicago, IL), and *P* < 0.05 was considered statistically significant. Secondary structures of aptamers were determined using free Internet-based Vienna RNA software (<http://rna.tbi.univie.ac.at/cgi-bin/RNAfold.cgi>) using DNA parameters at 25 °C.¹⁹

RESULTS AND DISCUSSION

SELEX is a classical technique to select DNA aptamers of target proteins.^{18,20} In this investigation, we selected a panel of aptamers to antitoxoplasma IgG using SELEX technology. The scheme of SELEX process is illustrated in Figure 1. In the selection process, monoclonal antitoxoplasma IgG antibody is adopted as the target template for aptamers selection, and a random ssDNA library with a capacity of 10⁵–10⁶ is constructed using asymmetric PCR. To improve the selection



Figure 1. Flowchart of the SELEX cycle for antitoxoplasma aptamer selection.

efficiency, the concentrations of antitoxoplasma IgG and ssDNA are optimized in each selection round. Detailed parameters adopted in the selection rounds are listed in Supporting Information Table 1. To ensure more ssDNA can combine to antitoxoplasma IgG, the initial concentrations of antitoxoplasma IgG and ssDNA are set as the highest in the first round of selection; so is the incubating time. Then, we reduce the concentrations of antitoxoplasma IgG and ssDNA gradually to increase the specificity of the aptamer via selective pressure.

An affinity diagram is built to determine the optimal SELEX rounds. Figure 2A shows that the absorbance increases linearly

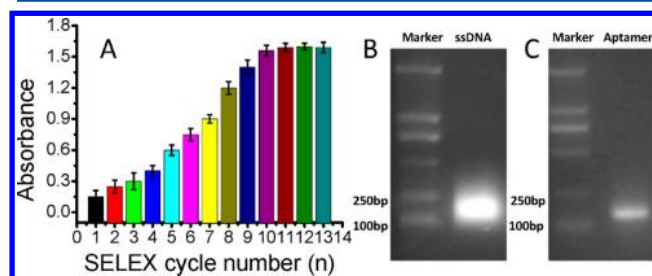


Figure 2. Affinity of selected aptamers with antitoxoplasma IgG. (A) Mean absorbance of the ssDNA acquired after different cycling number; *n* = 3. (B) Electrophoresis of the ssDNA obtained from the first round of asymmetric PCR amplification. (C) Electrophoresis of the selected aptamer after 10 rounds of screening. Marker: DL2000 marker.

until a plateau is reached at the 10th round, where a 7.2-fold increase to the initial concentration is observed. Because absorbance reflects the binding capability between aptamer and target protein, our results suggests that aptamers with high affinity to antitoxoplasma IgG have been successfully selected after round 10. These results are also confirmed using a gel electrophoresis (Figure 2, parts B and C), showing the aptamer band is much narrower and weaker (Figure 2C) than the original ssDNA library (Figure 2B). Although the amounts and the sequences have influence on electrophoresis band, the width of the band is mainly decided by the contents of the mixture. So we consider the narrower band means less ssDNA

Table 1. Basic Information of the Selected Aptamers

No.	Upper primer	Core sequence	Lower primer	Length	Absorbance	Minimum Free Energy
TGA4	GGGAGCTCAGAATAAAGCTCAACGCATTTCGCA	ACACAACCTGGCCAA	CGTTCCTGGTTCGACATGCGGCCGGATC	78bp	1.095	-13.40 kcal/mol
TGA6	GGGAGCTCAGAATAAAGCTCAACGCATTTCGCA	ACA CGC CTTGGC*AA	CGTTCCTGGTTCGACATGCGGCCGGATC	77bp	1.891	-17.80 kcal/mol
TGA7	GGGAGCTCAGAATAAAGCTCAACGCATTTCGCA	ACA TGA CTTCC*AA	CGTTCCTGGTTCGACATGCGGCCGGATC	77bp	2.129	-4.40 kcal/mol
TGA8	GGGAGCTCAGAATAAAGCTCAACGCATTTCGCA	ACACGACTTGGCCAG	CGTTCCTGGTTCGACATGCGGCCGGATC	78bp	1.102	-16.10 kcal/mol
TGA9	GGGAGCTCAGAATAAAGCTCAACGCATTTCGCA	ACACGACTTGGCCAA	CGTTCCTGGTTCGACATGCGGCCGGATC	78bp	1.376	-10.50 kcal/mol
TGA15	GGGAGCTCAGAATAAAGCTCAACGCATTTCGCA	ACACGACTTGACAAA	CGTTCCTGGTTCGACATGCGGCCGGATC	78bp	1.841	-13.40 kcal/mol
TGA20	GGGAGCTCAGAATAAAGCTCAACGCATTTCGCA	GCACGACTCGGCCAA	CGTTCCTGGTTCGACATGCGGCCGGATC	78bp	1.479	-17.20 kcal/mol

variation, suggesting almost all of the ssDNA molecules with low binding affinity have been removed. After cloning and identification, seven clones of aptamer with the highest affinity have been selected finally using the optimized SELEX protocol. The detailed sequences of these antitoxoplasma IgG aptamers (TGA) are listed in Table 1. It clearly shows that all of these seven aptamers have similar strand length (77 or 78 bp) and high affinities to antitoxoplasma IgG with absorbance ranging from 1.095 to 2.129. These aptamers share a common upper primer sequence and lower primer sequence; the variations only exist in the core sequence with a length of 14 or 15 bp. Theoretical secondary structures of these seven aptamers are estimated, using a dynamic programming algorithm of lowest free energy (Figure 3). Figure 3A shows that the secondary structures of these seven aptamers mainly contain stem-loops and half-ring structures.

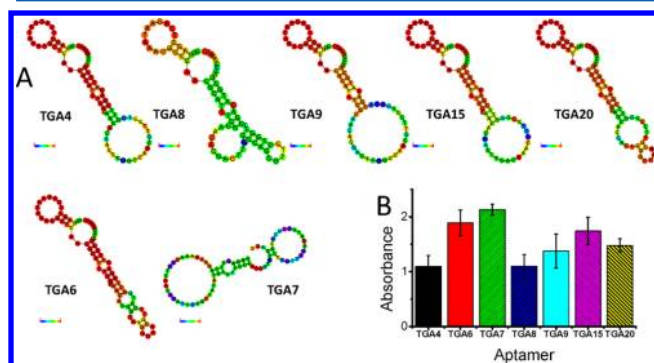


Figure 3. (A) Secondary structures of these seven aptamers. The structure below is colored by base-pairing probabilities. For unpaired regions the color denotes the probability of being unpaired. (B) The absorbance of different aptamers after 12 rounds of screening with antitoxoplasma antibody; $n = 3$.

Figure 3B shows the affinities of these selected aptamers with antitoxoplasma IgG. It clearly shows that the affinities of TGA6, TGA7, and TGA 15 are significantly higher than the other four aptamers. To simplify the analysis procedure, two aptamers (TGA6 and TGA7) with the highest affinities are selected as the aptamer probes for later biosensor construction. Table 1 shows that both TGA6 and TGA7 have identical length of 77 bp. The 77 bp long aptamer contains three sections: upper primer, lower primer, and the core zone. All of these seven aptamers share the same upper primer and lower primer. In the core sequence, four bases' differences are observed between TGA6 and TGA7: It is cytosine in TGA6, whereas it is thymine in TGA7 at the fourth base. It is guanine in TGA6 sequence, whereas it is adenine in TGA7 at the sixth base. It is guanine in the TGA6 and cytosine in TGA7 sequence at the 10th and the 11th base. Despite that only four-bases' differences are

witnessed, TGA6 and TGA7 demonstrate significantly different secondary structures.

It is predicted that TGA6 contains three small stem-loops and two big pockets structures, with a minimal free energy of -17.8 kcal/mol (Figure 3A). As for TGA7, two large pockets and one small stem-loop are found with a minimal free energy of -4.4 kcal/mol. Besides, the stem of TGA7 is much shorter than that of TGA6. Because binding affinity is mainly decided by the conformation, the relationships between binding affinity and secondary structure of aptamers can be derived accordingly. TGA7 has a higher binding affinity to antitoxoplasma IgG than TGA6, and TGA7 has one open-ring structure than TGA6 in the secondary structure; it is hypothesized that the stem-loop region is the potential binding position between aptamer and antitoxoplasma IgG. This hypothesis has been proved by previous researches showing that the stem-loop structure in the secondary structure is the potential binding area.^{21,22}

To verify the feasibility of TGA6 and TGA7 in detection, a Q-DAS biosensor that employs TGA6 and TGA7 as the probes is developed to detect antitoxoplasma IgG in serum samples (Figure 4A). Because of significantly different secondary

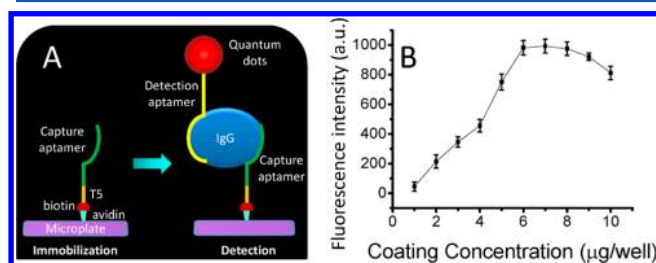


Figure 4. (A) Illustration of the detection principle of the quantum dots-labeled dual aptasensor. (B) Optimization of coating aptamer concentration; $n = 3$.

structure, these two aptamers naturally combine to different epitopes of antitoxoplasma IgG. Thus, a TGA6-IgG-TGA7 sandwich complex can be formed in the presence of antitoxoplasma IgG. The working principle of the Q-DAS is illustrated in Figure 4A. In a typical IgG detection protocol, biotin-modified aptamer TGA6 is immobilized in the micro-wells of a 96-well microplate to capture any antitoxoplasma IgG. After incubating the antitoxoplasma IgG solution with the microplate for 20 min, all antitoxoplasma IgG can be specifically captured on the surface of the microplate. Then QD-labeled detection aptamer (TGA7) is introduced to form a TGA6-IgG-TGA7 complex. After washing away any unbound aptamers, the TGA6-IgG-TGA7 complex that is tightly combined on the microplate can be measured using a fluorescent microplate reader. By this means, the emitted

fluorescent intensity of QDs is proportional to the concentration of captured antitoxoplasma IgG, guaranteeing the accurate and sensitive detection of antitoxoplasma IgG in a versatile setting. In the current setup, aptamers TGA6 and TGA7 can be interchangeable when being adopted as capture probe and detection probe due to their different binding epitopes. Semiconductor QDs are adopted as reporters in this research because QDs have extraordinary optical characteristics such as stronger quantum yield, antibleach feature, and narrower full width at half-maximum (fwhm) than traditional organic dyes such as Cy3 and TITC. QDs have been widely adopted in various immunoassays to increase the sensitivity of the assays.^{23–25} Our results also prove that the QD-labeled immunoassay can effectively improve the operating characteristics of the assay.

Probe density plays an important role in deciding the detection sensitivity and needs to be optimized.²⁶ Previous researches showed that higher probe density usually resulted in limited access and undesired steric crowding, while a lower density always provided a narrow linearity range.²⁷ Moreover, aptamer presents more serious steric hindrance than conventional ssDNA probe during the aptamer coating process, which is caused by the complicated secondary structure of aptamer that will inhibit aptamer immobilization. To eliminate the steric hindrance during the aptamer coating, a five base-pair long spacer (TTTTT) is added at the 5'-end of the aptamer probe according to ref 28. Results show that the spacer-modified probe provides higher sensitivity because of less steric hindrance (data not shown). In addition, we determine the optimal TGA6 coating concentration using a serial of concentrations ranging from 1 to 10 $\mu\text{g}/\text{well}$. Figure 4B shows that the fluorescence intensity in the proposed Q-DAS biosensor is proportional to the coated TGA6 concentration until a plateau is reached at 6 $\mu\text{g}/\text{well}$. Increased aptamer concentration induces decreased fluorescence response, which is mainly due to strong steric crowding effect of highly concentrated DNA hairpins on the surface. Meanwhile, the cost-effectiveness is significantly decreased due to the increased coating cost. Thus, 6 $\mu\text{g}/\text{well}$ is taken as the optimal aptamer coating concentration.

Owing to the design of the dual aptamer, the Q-DAS biosensor reflects a switch-on sensing mechanism that possesses preferable sensing properties. A previous dual-aptamer biosensor has already demonstrated preliminary applications in biomolecules detection. Compared with these previous dual-aptamer biosensors, the proposed Q-DAS biosensor provides improved sensitivity and feasibility due to the adoption of QD as the detection reporter. Under the optimized conditions described above, the detected fluorescence intensity of the aptasensor is proportional to the concentrations of antitoxoplasma IgG (Figure 5A). The inset of Figure 5A shows a good linear relationship, with a regression coefficient of 0.985 between the fluorescent intensity and the antitoxoplasma IgG concentration within the range from 0.5 to 500 IU. The regression equation is $Y = 225 \log X + 115$, where Y and X are the fluorescence intensity and IgG concentration, respectively. Antitoxoplasma IgG with higher concentration (above 500 IU) induces decreased regression coefficient, indicating the binding between immobilized aptamer and antitoxoplasma IgG has become saturated. Thus, any concentration higher than 500 IU needs to be diluted with PBS buffer prior to detection. Considering the common range of antitoxoplasma IgG in toxoplasmosis patients is lower than

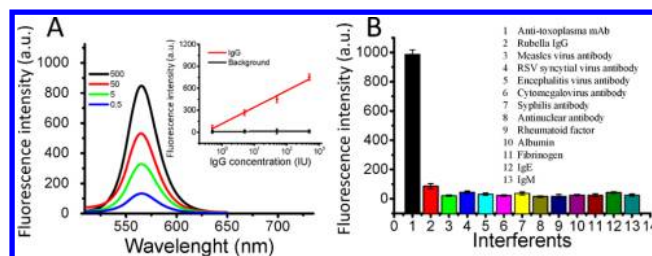


Figure 5. Fluorescence response of the quantum dots-labeled dual aptasensor (A). The inset denotes the calibration of Q-DAS for antitoxoplasma antibody detection. A linearity curve has been got within the range of 0.5–500 IU. (B) Specificity of the Q-DAS biosensor; $n = 3$.

400 IU, the linearity of 0.5–500 IU has covered the common range of antitoxoplasma IgG in blood.²⁹

The limit of detection (signal-to-noise ratio >3) is calculated by measuring the negative control for 20 consecutive duplicates. The limit of quantification is determined by serially diluting stocked antitoxoplasma IgG solutions with PBS buffer (pH 7.4). Five replicates were measured for the dilutions, and the final diluted concentration, which had a CV $<20\%$ between replicates, was considered the limit of quantification. Results show that the proposed Q-DAS biosensor has a limit of detection of 0.1 IU and a limit of quantification of 0.5 IU (CV = 7.8%). Thus, the sensitivity of the assay developed in this experiment is higher than those of traditional enzyme-linked immunosorbent assays (ELISAs) and other colloidal gold immunodot assay.³⁰

Specificity of the Q-DAS biosensor is determined using cross-reaction tests (Figure 5B), by adding several reported interfering agents (cytomegalovirus antibody, syphilis antibody, rubella antibody, antinuclear antibody, rheumatoid factor) and high-concentration proteins normally existed in the blood (albumin, fibrinogen, IgE, IgM). Results show that the fluorescence intensity induced by antitoxoplasma IgG is significantly higher than those from other proteins ($p < 0.05$). These weak, nonspecific signals may originate from the background interference caused by the autofluorescence of specific biomolecules in the serum matrix, which can be eliminated by introducing a reagent blank control consisting of the serum matrix. Previously reported false-positive reactions, resulted from antinuclear antibodies or rheumatoid factors in traditional IFA, are absent in the Q-DAS biosensor. These results suggest that the proposed Q-DAS assay is of extremely high specificities, benefited by the design of the dual-aptamer system. Traditionally, a single aptamer is adopted to perform the detection procedure, which is susceptible to the interference from other proteins and peptides. The adoption of two aptamers effectively increases the specificity of the assay; similar designs have been reported by using two monoclonal antibodies to construct high-throughput immunoassay or using two aptamers to conduct biosensor.^{31,32}

The accuracy of the proposed Q-DAS assay is determined by measuring the calibrators repeatedly at different intervals. Results show that mean intra-assay and interassay CVs are 3.48% and 8.63%, respectively. These results reveal that the storage time has considerable influence on the final fluorescent variability of the aptasensor. Considering conformational change is seldom occurred on the aptamer due to its short-chain DNA structure, the difference between the intra-assay and interassay mainly lies in the aggregation of QDs after long-

term storage, which leads to the attenuation of quantum yield of the QDs. To verify the influence of storage time on QDs fluorescence intensity, we measure the fluorescence intensity at different storage intervals. Result reveals that the carboxyl QDs solution can maintain its original fluorescence intensity for at least 2 months, while aptamer-modified QDs can only maintain their original fluorescence intensity for over 2 weeks. This finding suggests the aptamer–QD complex is less stable under long-term storage. The storage problem needs to be eliminated in future researches to make the QD-based assay meets most of the laboratory setting. Accuracy of the proposed Q-DAS biosensor is evaluated using recovery measurements. Results show that the recovery rates are 94.5%, 102.4%, and 96.3% for high, medium, low concentrations of antitoxoplasma IgG, respectively.

For methodology evaluation, we compare the results from proposed Q-DAS biosensor and Sabin–Feldman DT assay (the reference method). The ROC curve has been applied to determine the optimal positive cutoff value (Figure 6). When

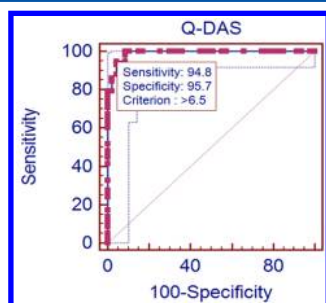


Figure 6. Result of clinical serum sample detection using the quantum dots-labeled dual aptasensor. When compared with the DT method, 183 from 189 (95.9%) negative samples are correctly reported, and 61 from 67 (91%) positive serums are correctly reported at the cutoff of 6.5 IU. Dotted line: 95% confidence interval (CI).

the optimal positive cutoff value is set as 6.5 ($P = 0.001$), there are 139 negatives and 6 positives in the DT negative group, with a negative detection rate of 95.9%. There are 6 negatives and 61 positives in the DT positive group, with a positive detection rate of 91.0%. These results show that the proposed dual aptasensor has extremely high specificity (95.7%), which is mainly contributed to the adoption of two aptamers. But the sensitivity of 94.8% still needs improving because any miss of detection within the pregnant women could be fatal. Decreasing the criterion is a feasible way to improve the sensitivity.

Figure 6 shows that the sensitivity almost reaches 100% once the cutoff value is set as 6.0, and the specificity can still be higher than 88%, ensuring the screening application during routine laboratory work. It has been widely reported that the discrepant results existed during different methodologies especially when the detected IgG values are low. Our findings also reveal the difficulties associated with interpreting serological results for low IgG values. These data highlight the benefit of using a confirmatory test to check samples with antitoxoplasma IgG titers close to the cutoff value.

CONCLUSIONS

This study, for the first time, successfully selected a panel of seven aptamers with high affinities to antitoxoplasma IgG using SELEX technology. By applying two aptamers (TGA6 and

TGA7) with the highest affinities as coating probe and detection probe, respectively, a Q-DAS biosensor is developed. The QD-labeled detection probe provides extraordinary fluorescence characteristics and significantly improves the sensitivity of the aptasensor. The proposed Q-DAS biosensor presents improved operating characteristics than conventional antibody-based assays, making it a promising candidate in clinical toxoplasma screening.

ASSOCIATED CONTENT

Supporting Information

Additional information as noted in text. This material is available free of charge via the Internet at <http://pubs.acs.org>.

AUTHOR INFORMATION

Corresponding Author

*E-mail: luoyang@tmmu.edu.cn (Y.L.); liaopu@sina.com (P.L.); weilingfu@yahoo.com (W.F.).

Author Contributions

[†]Y.L. and X.L. contributed equally to this work.

Notes

The authors declare no competing financial interest.

ACKNOWLEDGMENTS

This work is partly supported by Grants from the National Natural Science Foundation of China (81230064, 30900348), Natural Science Foundation of Chongqing (CSTC2013JJB10012), and Third Military Medical University (2010XZH08, WSS-2012-06).

REFERENCES

- (1) Montoya, J. G.; Liesenfeld, O. *Lancet* **2004**, *363*, 1965–1976.
- (2) Shapira, Y.; Agmon-Levin, N.; Selmi, C.; Petrikova, J.; Barzilai, O.; Ram, M.; Bizzaro, N.; Valentini, G.; Matucci-Cerinic, M.; Anaya, J. M.; Katz, B. S. P.; Shoenfeld, Y. *J. Autoimmun.* **2012**, *39*, 112–116.
- (3) Addebous, A.; Adarmouch, L.; Tali, A.; Laboudi, M.; Amine, M.; Aajly, L.; Rhajjaoui, M.; Chabaa, L.; Zougaghi, L. *Acta Trop.* **2012**, *123*, 49–52.
- (4) Rahbari, A. H.; Keshavarz, H.; Shojaee, S.; Mohebbi, M.; Rezaeian, M. *Korean J. Parasitol.* **2012**, *50*, 99–102.
- (5) Veronesi, F.; Ranucci, D.; Papa, P.; Branciarri, R.; Miraglia, D.; Moretta, I.; Caporali, A.; Pourquier, P.; Fioretti, D. P. *Large Anim. Rev.* **2012**, *18*, 65–70.
- (6) Zhang, H. S.; Thekisoe, O. M. M.; Aboge, G. O.; Kyan, H.; Yamagishi, J.; Inoue, N.; Nishikawa, Y.; Zakimi, S.; Xuan, X. N. *Exp. Parasitol.* **2009**, *122*, 47–50.
- (7) Ho-Yen, D. O.; Joss, A. W.; Balfour, A. H.; Smyth, E. T.; Baird, D.; Chatterton, J. M. *J. Clin. Pathol.* **1992**, *45*, 910–913.
- (8) Rigsby, P.; Rijpkema, S.; Guy, E. C.; Francis, J.; Das, R. G. *J. Clin. Microbiol.* **2004**, *42*, S133–S138.
- (9) Franck, J.; Garin, Y. J. F.; Dumon, H. *J. Clin. Microbiol.* **2008**, *46*, 2334–2338.
- (10) de Souza, G. F.; Carvalho, D.; Pedrosa, W.; Franck, J.; Piarroux, R. *Braz. J. Infect. Dis.* **2012**, *16*, 574–576.
- (11) Liesenfeld, O.; Press, C.; Montoya, J. G.; Gill, R.; Isaac-Renton, J. L.; Hedman, K.; Remington, J. S. *J. Clin. Microbiol.* **1997**, *35*, 174–178.
- (12) Safford, J. W.; Abbott, G. G.; Craine, M. C.; MacDonald, R. G. *J. Clin. Pathol.* **1991**, *44*, 238–242.
- (13) Jayasena, S. D. *Clin. Chem.* **1999**, *45*, 1628–1650.
- (14) Chen, F.; Hu, Y.; Li, D.; Chen, H.; Zhang, X. L. *PLoS One* **2009**, *4*, e8142.
- (15) Bruno, J. G.; Carrillo, M. P. *J. Fluoresc.* **2012**, *22*, 915–924.
- (16) Wang, B.; Guo, C.; Chen, G.; Park, B.; Xu, B. *Chem. Commun. (Cambridge, U. K.)* **2012**, *48*, 1644–1646.

- (17) Wang, C.; Hossain, M.; Ma, L.; Ma, Z.; Hickman, J. J.; Su, M. *Biosens. Bioelectron.* **2010**, *26*, 437–443.
- (18) Stoltenburg, R.; Reinemann, C.; Strehlitz, B. *Biomol. Eng.* **2007**, *24*, 381–403.
- (19) Gruber, A. R.; Lorenz, R.; Bernhart, S. H.; Neubock, R.; Hofacker, I. L. *Nucleic Acids Res.* **2008**, *36*, W70–W74.
- (20) Tok, J. B.; Fischer, N. O. *Chem. Commun. (Cambridge, U. K.)* **2008**, 1883–1885.
- (21) Luzi, E.; Minunni, M.; Tombelli, S.; Mascini, M. *TrAC, Trends Anal. Chem.* **2003**, *22*, 810–818.
- (22) Patel, D. J.; Suri, A. K.; Jiang, F.; Jiang, L.; Fan, P.; Kumar, R. A.; Nonin, S. *J. Mol. Biol.* **1997**, *272*, 645–664.
- (23) Michalet, X.; Pinaud, F. F.; Bentolila, L. A.; Tsay, J. M.; Doose, S.; Li, J. J.; Sundaresan, G.; Wu, A. M.; Gambhir, S. S.; Weiss, S. *Science* **2005**, *307*, 538–544.
- (24) Bogomolova, A.; Aldissi, M. *Biosens. Bioelectron.* **2011**, *26*, 4099–4103.
- (25) Freeman, R.; Liu, X.; Willner, I. *J. Am. Chem. Soc.* **2011**, *133*, 11597–11604.
- (26) Xiao, Y.; Lai, R. Y.; Plaxco, K. W. *Nat. Protoc.* **2007**, *2*, 2875–2880.
- (27) Opdahl, A.; Petrovykh, D. Y.; Kimura-Suda, H.; Tarlov, M. J.; Whitman, L. J. *Proc. Natl. Acad. Sci. U.S.A.* **2007**, *104*, 9–14.
- (28) Chang, C. C.; Lin, S. H.; Lee, C. H.; Chuang, T. L.; Hsueh, P. R.; Lai, H. C.; Lin, C. W. *Biosens. Bioelectron.* **2012**, *37*, 68–74.
- (29) Galanti, L. M.; Dell’Omo, J.; Wanet, B.; Guarin, J. L.; Jamart, J.; Garrino, M. G.; Masson, P. L.; Cambiaso, C. L. *J. Immunol. Methods* **1997**, *207*, 195–201.
- (30) Tracy, R. P. *Clin. Chem.* **2008**, *55*, 376–377.
- (31) Luo, Y.; Zhang, B.; Chen, M.; Jiang, T.; Zhou, D.; Huang, J.; Fu, W. *J. Transl. Med.* **2012**, *10*, 24.
- (32) Xie, S.; Walton, S. P. *Biosens. Bioelectron.* **2010**, *25*, 2663–2668.